Experimental Evidence for Electron Channeling in Fe/Au (100) Superlattices

D. T. Dekadjevi, P. A. Ryan, and B. J. Hickey
Department of Physics and Astronomy, E. C. Stoner Laboratory, University of Leeds, Leeds LS2 9JT, United Kingdom

B. D. Fulthorpe and B. K. Tanner
Department of Physics, University of Durham, South Road, Durham DH1 3LE, United Kingdom
(Received 23 May 2000)

We present transport and structural data from epitaxial (100) and (111) Au/Fe superlattices grown by molecular beam epitaxy. From their analysis, we conclude that an electron channeling mechanism, due to strong specular reflection of the minority spin carrier at the Au/Fe interfaces, is responsible for the high conductivity in the (100) superlattices.

DOI: 10.1103/PhysRevLett.86.5787 PACS numbers: 75.70.Cn, 73.40.–c, 73.50.–h, 75.70.Pa

The theory of the giant magnetoresistance (GMR) is still developing [1,2] and a number [3] of recent papers have interesting predictions about the nature of the electronic states in multilayers. In particular, the band structure that gives rise to spin-dependent scattering is thought to be responsible [4] for the spin-dependent confinement of electrons to specific layers within the system. A potential step can exist at the interface between the ferromagnetic layer and the nonmagnetic layer. This potential in the hybridized band structure affects the transmission of electrons through the interface. It should be possible, therefore, for electrons to scatter specularly from such an interface, and theoretical work has predicted the effect on the transport [5–10] and coupling properties in superlattices [11–13].

This type of specular reflection is quite distinct from that explored experimentally by Egelhoff *et al.* [14], Swagten *et al.* [15], and Yuasa *et al.* [16] where electrons are specularly scattered from an insulator or noble metal/vacuum interface. In true channeling the electron is confined to a layer within the material as a result of the band structure. States are completely reflecting if there are no states in the other material with the same parallel momentum. Additionally, at points of high symmetry, the effectiveness of coupling between s-p states of the spacer and the d states of the ferromagnet become important and lead to high reflection probabilities that are different for majority and minority carriers. When the magnetic moments in adjacent layers are parallel, one spin can have a high specular reflection coefficient at both interfaces and the spacer acts as an electron waveguide. If this spacer has a significantly lower resistivity than the magnetic layer, the channeled electrons will act as a low resistance shunt and thus enhance the GMR. In the antiparallel state, there is no confinement in the Au spacer.

According to the theory of Stiles [7], the Fe/Au (100) system is a good candidate in which to observe electron channeling. The probabilities for transmission *into* the Fe from the Au are 67% higher for majority carriers compared to the minority carriers. For transmission *from* the Fe into the Au, the majority carriers have a 21% higher probability of transmission. On the other hand, the minority electrons are largely confined to each material. The orientation between the successive magnetic moments in a multilayer greatly affects the channeling. Only in the saturated state where all magnetic moments are aligned can the channeling occur. Also, the channeling is related to the symmetry of the Fermi surface and therefore to the epitaxial relationship in the superlattice. Large channeling effects are predicted for (100) Fe/Au, whereas the Fe/Au(111) system is not expected to exhibit channeling as the band mismatch is so large [17].

In this Letter, we present experimental evidence for this mechanism in (100) oriented Fe/Au multilayers grown by molecular beam epitaxy [18]. The key experiments involve the study of the variation of conductivity and structural perfection as a function of the thickness of the Au layers. Fe/Au multilayers consisting of 20 repeats of a [Fe(10 Å)/Au(X)] structure, where X represents a thickness between 5 and 70 Å, were grown on a 50 Å Au buffer layer. *In situ* reflection high-energy electron diffraction (RHEED) measurements and high resolution x-ray diffraction data from Bragg planes parallel to the surface showed that multilayers grown on polished (100) faces of MgO (with a 10 Å Fe seed layer) were epitaxial with (100) orientation, while those grown on $(11\bar{2}0)$ sapphire (with a 30 Å Nb seed layer) were (111) oriented. The existence of superlattice satellites up to the seventh order around the 200 and 111 x-ray Bragg peaks for the respective systems showed that the interfaces were extremely sharp. Analysis of the diffraction peak widths in reciprocal space scans of 30 Å bilayer samples gives a lower limit to the out-of-plane subgrain size of 150 ± 20 Å and 570 ± 50 Å in the (100) and (111) systems, respectively. In these samples, for both orientations, there are many interfaces contained within each subgrain. It is important for the transport data presented later to note that we find the out-of-plane structure for the (111) samples to be of much higher quality than the (100) samples.

Oscillations, as a function of Au spacer thickness, in GMR (measured using a four-probe dc method at 4.2 K) and in the remanent magnetization were observed in the (100) orientation only. Our measured values of 15 ± 2 Å

and 7 ± 2 Å for the period of the exchange coupling compare well with predicted values of 17.2 Å and 5.0 Å [19] and those determined elsewhere [20,21]. However, the decay length of the coupling strength, as a function of spacer, thickness was unusually long. Several theoretical papers have predicted that the amplitude of exchange coupling is a function of the extent of electron confinement [11–13]. There was no coupling observed in the (111) samples and a maximum GMR of only 6% was found compared to 40% for the (100) samples with antiferromagnetic coupling. The residual resistivity ratios for our Fe/Au systems are typical of multilayers [22] and depend on Au thickness for both orientations. The values for Au layers less than 2 nm are 2 for (100) and 1.4 for (111) and for the thicker samples with Au of 6 nm we found 3.4 for (100) and 1.9 for (111).

The conductivity at 4.2 K, measured in a saturating magnetic field of 1 T, as a function of Au spacer thickness is shown in Fig. 1. The conductivity of a single bilayer of [Au(1000 Å)/Fe(10 Å)] has been measured as 0.88 ± $0.05(\mu\Omega\,\mathrm{cm})^{-1}$ in the (100) orientation and 0.73 ± $0.04(\mu\Omega\,\mathrm{cm})^{-1}$ in the (111) orientation. It is immediately apparent that the data from Fig. 1 should saturate, for large Au thickness, at roughly the same value, i.e., the conductivity of thick Au. We have found that while the (111) data can be explained in the Fuchs-Sondheimer model [23], the (100) data cannot, for any reasonable values of the Fe or Au conductivities. If electrons were to traverse many layers without scattering, the conductivity would depend on the average scattering properties of many Au and Fe layers and would not vary strongly with the thickness of the Au(100) spacer. However, if electron channeling exists in the (100) Au spacers, the mean-free path of the specularly reflected electrons may be long, leading to a high conductivity, without electrons crossing a large number of layers. The number N, of specular reflections prior to diffusive scattering at the Fe/Au interface, is determined by the potential step at the interface and does not change with Au thickness. Provided the mean-free path in the Au layer, λ_{Au}, is greater than the thickness of the Au, the mean-free path is directly proportional to the product of the number of specular reflections and the Au thickness: $\lambda_{\mathrm{Au}} \propto N t_{\mathrm{Au}}$. The total conductivity, σ, measured in plane is then the thickness-weighted sum of the conductivities of the individual Fe and Au layers, namely,

$$\sigma = \frac{20\zeta N t_{\mathrm{Au}}^2}{t_{\mathrm{tot}}} + \frac{20 t_{\mathrm{Fe}}}{t_{\mathrm{tot}}}\,\sigma_{\mathrm{Fe}}\,, \qquad (1)$$

where t_{Au} and t_{Fe} are the thicknesses of Au and Fe layers, t_{tot} is the total multilayer thickness, σ_{Fe} is the conductivity of the Fe layers, and ζ represents the usual constants from the Drude formula. Solid lines in Fig. 1 represent fits using Eq. (1) assuming that ζ is the same for all samples, independent of Au thickness and multilayer orientation. The only free parameter is the value of N and we find that the ratio of specular reflection coefficients between orientations N_{100}/N_{111} is 2.7 ± 0.1 with N_{100} equal to 9.

To go beyond this phenomenological model which assumes a spin-independent electron confinement, we have used the semiclassical model proposed by Hood and Falicov [4] to determine the saturation conductivity in an infinite [Fe(10 Å)/Au(X Å)] multilayer as a function of X. The conductivity has been calculated with and without specular reflections assuming spin-dependent scattering probabilities in the bulk and at the interfaces.

The spin-dependent relaxation time and potential of the layer were varied to keep the conductivity equal to that measured in the bulk. At the interface, three possible cases are distinguished: transmission (T), specular reflection (R), and diffuse scattering (D), where $T + R + D = 1$. The values of T and R are determined by the layer potentials and D was set as 0.3 for all layers. We have set the potential of the Au layer in agreement with the free electron value of the Fermi energy. In order to confine the electrons, the potential in the Fe must be varied. As expected, free electron values of the Fermi energy for Fe do not work and, therefore, to introduce confinement in the Au, the potentials for majority and minority carriers in Fe are changed in order to reproduce the value of R and T predicted by Stiles.

Within the model we find that without electron confinement the (100) Au conductivity must be 25 times higher than the (111) Au to explain the experimental data. This is unreasonable considering the structural data and the measured conductivities. We therefore fixed the conductivities of layers in each orientation to be equal to the measured values and then switched on the channeling for the (100) samples. The results are shown as squares in Fig. 1. The agreement with the experimental data is very good when the probability of specular reflection is set to 0.6 for minority electrons and 0.3 for the majority electrons, which is close to the values predicted by Stiles [7]. We also found that varying D, the diffuse scatter at the interface, could not

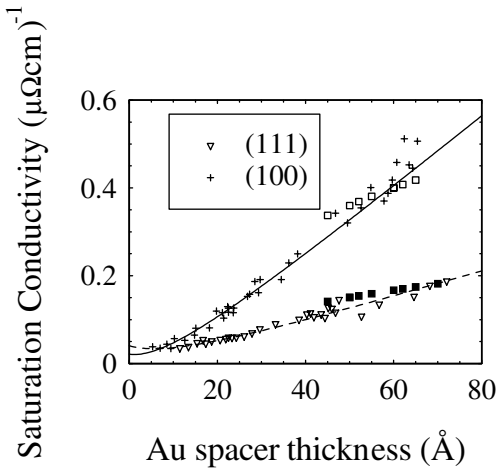

FIG. 1. Saturated conductivity as a function of spacer thickness for (100) (crosses) and (111) (triangles) [Fe(10 Å)/Au(X)]$_{20}$ superlattices at 4.2 K. Lines represent fits of Eq. (1). Also shown is the saturation conductivity calculated using the semiclassical model of Hood and Falicov for (100) (open squares) and (111) (solid squares).

account for the data. We conclude, therefore, that channeling is required to explain the observed differences in the conductivity of (100) and (111) superlattices.

We have undertaken extensive structural measurements to demonstrate the validity of the above analysis which assumes no significant change in the structural quality of the samples with Au thickness. In-plane diffraction measurements have been carried out *in situ* using reflection high-energy electron diffraction and *ex situ* using grazing incidence x-ray diffraction (GIXD). To perform an *in situ* RHEED analysis, the growth of an 80 Å Au layer on 10 Å of Fe has been interrupted at different stages. The patterns exhibit fine and continuous streaks characteristic of a 2D well ordered Au surface, which is expected from the difference of free surface energy of the materials. The full width at half maximum (FWHM) of the streaks is a measure of the in-plane coherence length. As can be seen in Fig. 2, this was found to be constant in both of the orientations for Au layers thicker than 30 Å, where the conductivity in Fig. 1 shows significant dependence on the Au thickness. For thick Au, the coherence length of the (111) samples was slightly larger than the (100).

Grazing incidence x-ray diffraction experiments have been performed on BM28, the XMaS CRG beam line, at the European Synchrotron Radiation Facility in Grenoble. In the GIXD geometry, the diffracting planes are perpendicular to the sample surface and the diffraction peaks measured by rotation of sample and detector about the normal to the surface. It is therefore sensitive to in-plane structure and disorder in the Au and Fe layers. Use of a grazing angle of the incident beam below the critical angle (in our experiments 0.2°) limits the depth sensitivity to approximately 30 Å. The FWHM of the in-plane θ-2θ scans are 0.5°–0.8° for the (111) and 0.2° for the (100) orientation samples, respectively. Figure 3 shows θ scans of scattered intensity as a function of the specimen angle about its surface normal taken with the detector at the Au (022) reflection position. The four- and sixfold symmetries show the Au layers to be deposited with well-defined (100) and (111) orientation in the MgO and sapphire systems, respectively. The FWHM of the peaks of Fig. 3 provides a direct measure of the mosaic width of in-plane crystalline disorder. For the (100) samples, the mosaicity width was found to vary from 0.49° to 0.47° for Au layer thicknesses between 35 and 70 Å, whereas for (111) the widths varied from 2.35° to 2.02°. The absence of variation of rocking curve FWHM with thickness in the (100) samples is strong evidence against defect scattering being responsible for the change in the conductivity [24]. High angle x-ray diffraction rocking curves of these samples [25] show that the in-plane scattering domain (subgrain) size of the (111) orientation is about 2–3 times that of the (100) orientation. The lower conductivity of the (111) samples cannot therefore be attributed to increased grain boundary scattering.

The specular reflectivity data show Kiessig fringes and Bragg peaks for both (100) and (111) epilayers, and the nominal thickness was found to be in good agreement with that deduced from the x-ray results. Kiessig fringes and Bragg peaks were also observed in the off-specular radial scans, indicating that a large proportion of the interface roughness is correlated (conformal) through the multilayer. The thickness of individual layers, the electron density gradient, conformal and random roughness, in-plane roughness correlation length (ξ), and Hirst fractal parameter, h, were obtained by matching the experimental data to that simulated for a fractal model structure within the distorted wave Born approximation [26,27]. Excellent agreement is found between experimental and simulated data for transverse (q_y) scans, with good reproducibility between samples. For the (111) Fe/Au epilayers grown on sapphire we find (Fig. 4a) that the interface roughness is highly correlated in nature with a correlated-to-uncorrelated roughness ratio close to 16:1. The lateral correlation length, ξ, is determined to be 250 ± 20 Å with a fractal Hirst parameter $h = 0.20 \pm 0.05$. The (100) Fe/Au grown on MgO also exhibits an interface roughness which is highly correlated in nature. Matching of simulated and experimental data (Fig. 4b) yields a correlated-to-uncorrelated roughness ratio of 10:1 and a lateral correlation length $\xi =$ 250 ± 20 Å, with a fractal parameter $h = 0.28 \pm 0.05$. As the fractal parameter varies from 0 to 1 on moving from

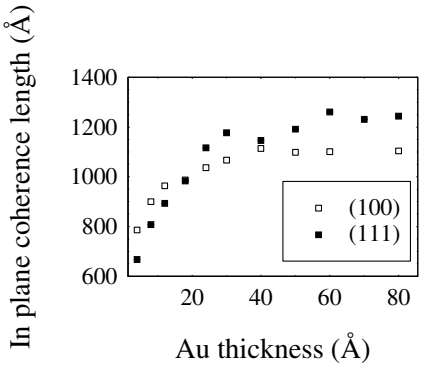

FIG. 2. In-plane coherence length, determined from the width of RHEED streaks, as a function of the Au thickness and of the orientation.

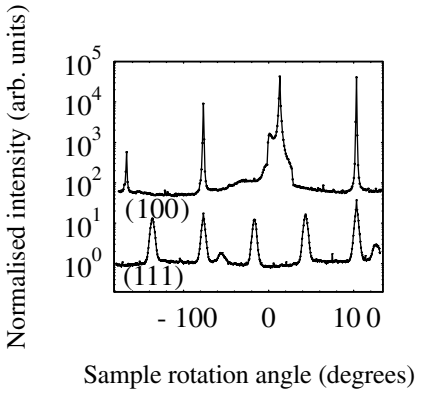

FIG. 3. GIXD measurements of the in-plane rocking curves of the Au 022 reflection for a (100) sample of Au layer thickness 12 Å and a (111) orientation multilayer of Au thickness 20 Å.

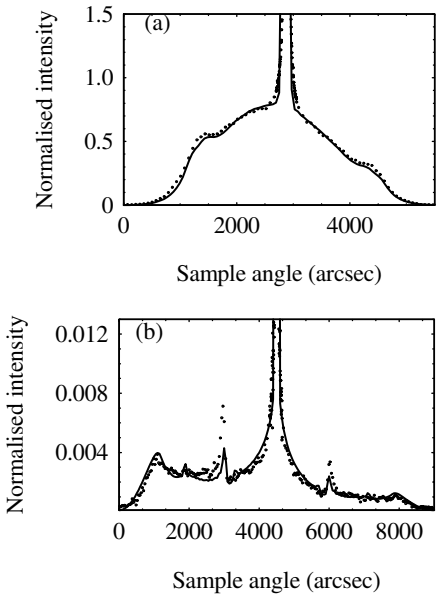

FIG. 4. Grazing incidence x-ray transverse diffuse scan for Fe/Au (100) on MgO (a) and (111) on sapphire (b) with an x-ray wavelength $\lambda = 1.03$ Å. Experimental data shown by points, simulated fit by the solid line. [The intensity differences arise from the differing scattering angles in (a) and (b).]

a three to a two dimensional surface, within the experimental error there is no difference in dimensionality between the two orientations. In all layers measured, the rms amplitude of the roughness in the (100) system is almost 3 times that of the (111) system, (9.3 $\pm$ 0.2 Å compared with 3.3 $\pm$ 0.2 Å). The interface morphology is found to stay the same when varying the Au thickness. The interface width deduced from the specular scatter equaled the roughness determined from the diffuse scatter, showing that interdiffusion was negligible. Therefore, these structural properties imply that the (111) system should have the higher conductivity, contrary to the observations.

The values of σ_{Fe}, determined from the intercept in Fig. 1, are very similar in the (111) and (100) materials. GIXD measurements indicate that the (100) Fe is in good crystallographic registration with the (100) Au as expected from the lattice matching. *In situ* RHEED data [28] and *ex situ* medium energy ion scattering [29] experiments from multilayers grown on sapphire showed that the growth of Fe (111) on Au(111) is pseudomorphic for Fe thicknesses less than 10 Å in agreement with previous results [30]. The (111) Fe/Au system eventually relaxes into its bulk structure, but only after the Fe thickness becomes greater than 15 Å. For all samples in this study, therefore, both orientations grow epitaxially.

The structural studies show that neither the variation of the saturation conductivity as a function of Au layer thickness nor the difference between (100) and (111) oriented multilayers can be attributed simply to the difference in sample quality. We thus conclude that the data in Fig. 1 demonstrate the existence of electron channeling in Fe/Au (100) multilayers.

We thank M. Horlacher for coding the Hood and Falicov model, J. Xu for some of the resistivity measurements for the (111) samples, and M. A. Howson and W. P. Pratt for valuable discussions. The helpful and friendly assistance at the ESRF of T. P. A Hase and XMaS beam line members S. D. Brown, D. F. Paul, A. Stunault, and P. Thompson and financial support from the Engineering and Physical Science Research Council are gratefully acknowledged.

[1] D. Bozec *et al.,* Phys. Rev. Lett. **85**, 1314 (2000).
[2] A. Brataas, Yu. V. Nazarov, and G. E. W. Bauer, Phys. Rev. Lett. **84**, 2481 (2000).
[3] W. H. Butler, X-G. Zhang, and J. M. MacLaren, J. Supercond. **13**, 221 (2000); T. C. Schulthess *et al.,* Phys. Rev. B **56**, 8970 (1997); X-G. Zhang and W. H. Butler, Phys. Rev. B **51**, 10 085 (1995); E. Yu. Tsymbal and D. G. Pettifor, Phys. Rev. B **61**, 506 (2000); J. Magn. Magn. Mater. **202**, 163 (1999); Phys. Rev. B **54**, 15 314 (1996); S. Sanvito, C. J. Lambert, and J. H. Jefferson, Phys. Rev. B **60**, 7385 (1999).
[4] R. Q. Hood and L. M. Falicov, Phys. Rev. B **46**, 8287 (1992).
[5] W. H. Butler *et al.,* Phys. Rev. Lett. **76**, 3216 (1996).
[6] S. Zhang and P. M. Levy, Phys. Rev. B **57**, 5336 (1998).
[7] M. D. Stiles, J. Appl. Phys. **79**, 5805 (1996).
[8] A. Vedyayev *et al.,* J. Phys. Condens. Matter **5**, 8289 (1993).
[9] B. R. Bulka and J. Barnas, Phys. Rev. B **51**, 6348 (1995).
[10] K. M. Schep *et al.,* J. Magn. Magn. Mater. **177**, 1166 (1998).
[11] J. Mathon *et al.,* J. Magn. Magn. Mater. **121**, 242 (1993).
[12] M. D. Stiles, Phys. Rev. B **48**, 7238 (1993).
[13] P. Bruno, Phys. Rev. B **52**, 411 (1995).
[14] W. F. Egelhoff *et al.,* J. Vac. Sci. Technol. B **17**, 1702 (1999); W. F. Egelhoff *et al.,* IEEE Trans. Mag. **33**, 3580 (1997).
[15] H. J. M. Swagten *et al.,* Phys. Rev. B **53**, 9108 (1996).
[16] S. Yuasa *et al.,* J. Appl. Phys. **83**, 7031 (1998).
[17] M. D. Stiles (private communication).
[18] M. A. Howson *et al.,* J. Phys. Condens. Matter **11**, 5717 (1999); J. Xu *et al.,* J. Appl. Phys. **81**, 3908 (1997).
[19] P. Bruno and C. Chappert, Phys. Rev. Lett. **67**, 1602 (1991).
[20] K. Shintaku, Y. Daitoh, and T. Shinjo, Phys. Rev. B **47**, 14 584 (1993).
[21] J. Unguris, R. J. Celotta, and D. T. Pierce, J. Appl. Phys. **75**, 6437 (1994).
[22] M. Suzuki and Y. Taga, Phys. Rev. B **52**, 361 (1995); E. E. Fullerton *et al.,* Phys. Rev. B **48**, 15 755 (1993).
[23] See K. L. Chopra, *Thin Film Phenomena* (McGraw-Hill, London, 1969).
[24] A. R. Modak, D. J. Smith, and S. S. P. Parkin, Phys. Rev. B **50**, 4232 (1994).
[25] B. D. Fulthorpe *et al.,* J. Phys. D **34**, A203–A207 (2001).
[26] T. P. A. Hase, I. Pape, M. Wormington, and B. K. Tanner, Physica (Amsterdam) **253B**, 278 (1998).
[27] S. Sinha *et al.,* Phys. Rev. B **38**, 2297 (1988).
[28] D. T. Dekadjevi *et al.* (to be published).
[29] T. C. Q. Noakes *et al.,* Phys. Rev. B **58**, 4934 (1998).
[30] J. A. Stroscio *et al.,* J. Vac. Sci. Technol. A **10**, 1981 (1992).